Masking mechanisms applied to thin-film coatings for the manufacturing of linear variable filters for two-dimensional array detectors

Laëtitia Abel-Tibérini,* Frédéric Lemarquis, and Michel Lequime

Institut FRESNEL, UMR CNRS 6133, Université Paul Cézanne—Ecole Centrale Marseille—Université de Provence, Domaine Universitaire de Saint-Jérôme, 13397 Marseille Cedex 20, France

*Corresponding author: laetitia.abel@fresnel.fr

Received 3 June 2008; revised 27 August 2008; accepted 15 September 2008; posted 22 September 2008 (Doc. ID 96993); published 17 October 2008

We propose a method for manufacturing linear variable interference filters for two-dimensional (2D) array detectors, based on the use of correcting masks combining both rotation and translation movements of the masks and substrates. The major advantage of this method is its capability to produce several identical filters in a single run. 20 mm × 20 mm samples were manufactured with a wavelength ratio almost equal to 2 along the thickness gradient direction. In agreement with calculations, the measured uniformity perpendicular to the gradient is about 99.8% along 20 mm.

OCIS codes: 310.1860, 310.6860.

1. Introduction

Based on interference phenomena, the major parameter for thin-film optical coatings is the ratio between the wavelength and the thickness of each layer. According to the thickness chosen for each layer, many optical functions can be designed with different transmittance or reflectance spectral responses, such as antireflection coatings, edge filters, and bandpass filters. The counterpart for this flexibility is that the optical response of a coating is potentially subject to a spatial evolution along the surface of the substrate if the thickness of each layer happens not to be perfectly uniform [1]. For the sake of simplification, we consider that the thickness nonuniformity is identical for all the materials involved in the coating—in that case, only a wavelength shift of the optical properties can be observed, depending on the point considered at the surface of the component. Except for achromatic designs, such as broadband beam splitters or antireflection coatings where this phenomenon is not critical, most often this wavelength shift has to be canceled or, at least, minimized. However, depending on the aim, applications exist that demand components with optical properties that change continuously from one point to another, such as variable coatings designed for laser beam shaping or linear variable filters for spectroscopy [2,3]. As far as laser beam shaping is concerned, there is only one single wavelength for which the intensity or phase properties must be controlled with circular geometry. In such a case, the coating is usually designed using just a few nonuniform layers, for example, a nonuniform spacer layer inside a uniform Fabry–Perot cavity. On the contrary, a linear variable filter is designed as a band pass structure in which all the layers are affected with the same thickness nonuniformity, i.e., with linear geometry. As a result, the centering wavelength of the filter shifts along the direction corresponding to the thickness gradient.

This property is very interesting for spectroscopic applications since such coatings can be imaged on, or placed directly in front of, linear array (or 2D array) detectors to design light and compact spectrometers,

0003-6935/08/305706-09$15.00/0

each pixel (or line) being addressed with a particular wavelength [4]. In addition, due to the absence of any moving part, such systems should be highly reliable and all these advantages are greatly appreciated for space instrumentation.

For such a spectrometer, the Paris–Meudon observatory asked us to study the manufacturing of a linear variable filter for a 2D array detector [5]. Like linear array detector coatings, these films' thickness distribution must provide the correct wavelength shift along the spectral direction. But in the case of 2D array detectors, such as CCD matrices, a near-perfect thickness uniformity also has to be maintained perpendicular to this direction so that each column of the detector is addressed with a single wavelength. This second point, which is the main topic of this paper, is much more difficult to fulfill than the first one, mainly because of the natural nonuniformity of the deposition process which must be taken into account.

As will be detailed in Section 4, one consequence is that it is difficult to manufacture several filters in the same deposition run and masking systems are developed and optimized for the manufacturing of one coating at a time [6]. To solve this problem, we developed a mechanism using correcting masks and combining both a rotation and a translation movement of these masks, using a came. This mechanism allows the simultaneous manufacturing of several samples with a minimum of 99.8% transverse uniformity, which is compliant with standard requirements. Moreover, this transverse uniformity is nearly independent of the natural thickness distribution of the coating machine. This result was confirmed experimentally using a dual ion beam sputtering process.

Section 2 is devoted to the numerical model we used to calculate the film thickness distribution, taking into account the deposition machine geometry, as well as the shapes and movements of the mask and of the sample. Sections 3 and 4 will describe the results that can be obtained using only either a rotation or a translation movement. Section 5 will describe the result that can be obtained when combining these two elementary movements, and Section 6 will present experimental results that confirm theoretical ones regarding the transverse uniformity of the coatings.

2. Thickness Distribution Model

To deposit nonuniform layers, the most frequent solution consists in using mechanical masks. However, the precise determination of both the shape of these masks and their relative movements with the substrates to be coated is difficult and time consuming if performed only through experimental tests. As a consequence, we developed a numerical model which helped us first to define, and eventually optimize, these geometrical parameters with a limited number of experimental trials. Figure 1 schematically represents the geometry of the dual ion beam sputtering machine we used for this study. In its classical configuration, the substrate holder rotates horizontally.

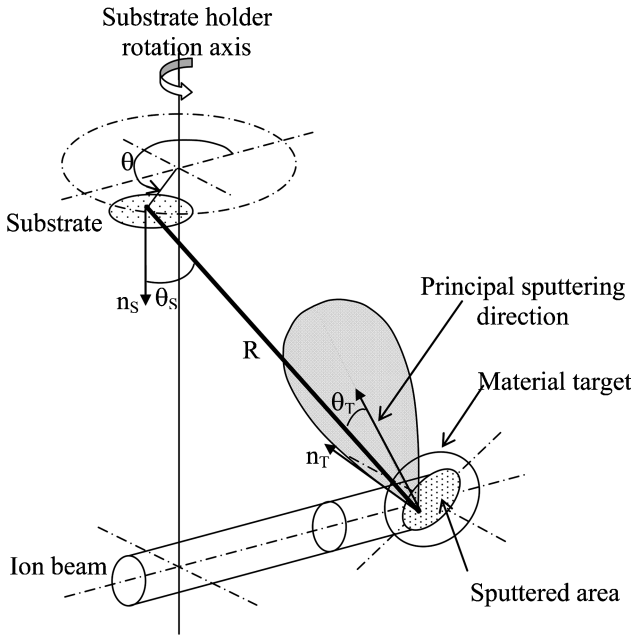

Fig. 1. Representation of the sputtering machine geometry used for the calculation and manufacturing of the linear variable filters.

The angle between the horizontal plane and the material target is 45°. The axis of the sputtering ion beam is horizontal, reaching the center of the material target through the rotation axis. As a consequence, the projection of the ion beam on the material target defines an elliptical area that corresponds to the effective material source and the relevant parameter for the target size is not the size of the material target itself, but the diameter of the ion beam. In the software we developed, the angles defining the position of the target and the incidence of the ion beam are free parameters; as a consequence, it can also be used to simulate an evaporation process, considering a horizontal material target with a fictive vertical ion beam to define a circular material source.

A. Thickness Calculation Without Masks

Considering one point on the material target and one point on the substrate, the elementary amount of deposited material is classically assumed proportional to the quantity

$$\cos\theta_S \cos^a\theta_T / R^2, \tag{1}$$

where θ_S and θ_T, respectively, represent the angles between the line joining these two points and the normal vectors to the substrate ($\vec{n}_S$) and to the material target ($\vec{n}_T$), R being the distance between the two points [1,7]. Parameter a is linked to the process directivity. This formula is usually given for an evaporation process where the evaporated material is distributed with radial symmetry around the normal vector to the material source. However, considering a sputtering process, the main sputtering direction is not necessarily normal to the material surface but

depends on the ion beam energy as well as on the ion beam incidence angle [8,9]. As a consequence, as illustrated in Fig. 1, we consider in our model that the angle θ_T is determined using not the normal vector but the main sputtering direction as reference. In our model, this direction belongs to the plane defined by the target and the rotation axis and is characterized by its angular deviation from the normal vector of the target surface.

To complete this model, each point of the material target is weighted with a coefficient representing the energy profile of the ion beam, which is assumed to be a Gaussian one. For this purpose, in addition to the diameter of the ion beam, it is necessary to give the percentage of energy, b, corresponding to this diameter. For any point of the material source, the weighting coefficient is then given by

$$W(r) = e^{r^2/2d^2 \mathrm{Ln}(b)}, \tag{2}$$

where r and d, respectively, represent the distance from this point to the axis of the ion beam and the diameter of the ion beam.

To calculate the total amount of material deposited on one point of the sample, one must perform the integral of the deposited differential thickness for the complete surface of the material source and during the complete trajectory of the sample—or at least during one period, since the movement is generally periodic. This summation is performed numerically considering a hexagonal sampling of the material target.

Finally, to calculate the coating thickness uniformity, the deposited thickness is calculated for each point of the substrate and normalized with respect to the maximum value. The sampling of the substrate surface is performed with a rectangular grid.

For the calculations illustrating the model in this paper, we used 135 points for the material target and 400 points for the substrate. The angular step for the rotation of the substrate holder is 0.5° and calculations were performed over one complete revolution.

The parameters corresponding to the geometry of our deposition machine are as follows:

– the height of the substrate is 230 mm (from the center of the material source) and
– the distance between the rotation axis and the center of the material source is 125 mm.

We used 20 mm square substrates placed on the rotating substrate holder at radius 50 mm.

As already mentioned, the size of the material source, the sputtering direction, the sputtering directivity, and the amount of sputtered material depend on both the material and the sputtering ion beam characteristics. In this paper, we will consider the following characteristics:

– the diameter of the ion beam is 125 mm,
– the amount of sputtered material for this diameter is characterized by $b = 0.06$ [see Eq. (2)],
– the angle between the sputtering direction and the normal vector perpendicular to the material source is 15°, and
– the sputtering directivity is given by $a = 1$ [see Eq. (1)].

These values result from preliminary tests performed recently concerning the thickness distribution characterization of Ta_2O_5. For this characterization, a Ta_2O_5 single layer was deposited on a large 250 mm × 180 mm static glass window on which a thickness and index characterization mapping was performed. Coupled with the thickness distribution model described above, a nonlinear simplex optimization algorithm was used to determine these deposition parameters. Table 1 gives the ratio between measured and calculated uniformity. The discrepancy is most often below 1%, while the thickness range extends from 1550 to 3850 nm. A similar near-correspondence was also obtained using rotating substrates. All these characterization results will be detailed in a specific paper.

B. Introduction of Masks

Masks are assumed to belong to a horizontal plane. They can be defined by closed lines of two types: polygonal shapes given by the list of the corners coordinates or curved shapes given by a polar Fourier development. One can define which part of the mask, internal or external, is empty. In order to define more complex mask shapes, one can define logical operations between elementary masks, such as union or intersection, as illustrated in Fig. 2, which represents a mask that will be used in Section 3. Each mask is given its own position and movement law. Standard movements are rotation and translation. Section 5 will give the example of a mask movement combining both.

Including the effect of the masks in the calculation of the thickness uniformity implies calculating the positions of the masks and of the substrate for each motion step. Then, for each line joining one point of the substrate to one point of the material target, one must determine the intersection coordinates of this

Table 1. Mapping of the Uniformity Mismatch Between Calculated and Measured Values Obtained for a Ta_2O_5 Single Layer Deposited on a 250 mm × 180 mm Static Substrate[a]

Coordinates (mm)	37	2	−33	−75	−117	−166
−79	1.0236	1.0115	1.0039	1.0033	1.0135	1.0746
−44	1.0128	1.0044	1.0029	1.0039	1.0003	1.0180
−12	1.0024	1.0068	1.0028	1.0026	1.0011	1.0026
30	1.0023	1.0019	1.0016	1.0045	1.0018	1.0019
76	1.0128	1.0062	1.0041	1.0001	1.0092	1.0083

[a]The figures in the table correspond to the ratio between the measured uniformity and the calculated one after numerical optimization of the deposition parameters used in the "thickness distribution model." Point coordinates are referenced with respect to the rotation axis of the machine (0, 0).

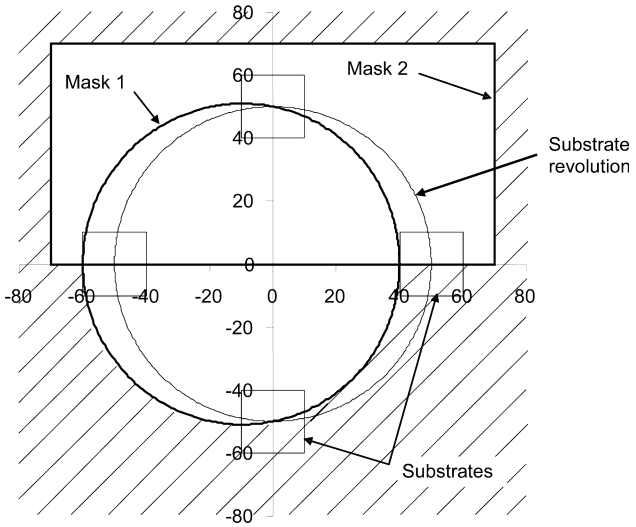

Fig. 2. Definition of a static masking geometry for the deposition of linear variable filters. The mask is formed by the union of a curved one (mask 1) and a polygonal one (mask 2) so that the rotating substrate is progressively hidden during half a turn.

line with the masks' planes and determine if the resulting intersection points correspond to the internal or external parts of the masks. Then, depending on the result of the logical operation defined with these masks, we can decide whether the corresponding elementary thickness amount must be taken into account.

3. Deposition of Linear Variable Filters Using a Rotation Movement

To manufacture graded coatings, the easiest configuration—requiring no complex modification in a standard deposition chamber—simply consists of using the rotation movement of the substrate holder combined with a static mask placed just below the substrates. Figure 2 shows the shape of such a mask and its relative position to the substrate. Notice that, as described in Subsection 2.A, this mask is formed by two elementary masks, a curved and symmetrical one completed by a large rectangular one which permits keeping only one half of the first one. During one half of the revolution, the substrate is completely exposed to material deposition, while during the other half, the substrate is gradually hidden behind the mask, its external side being always hidden while its internal side is never hidden. As a consequence, this kind of mask approximately gives on the internal side of the substrate twice the thickness deposited on the external one.

For calculation, the curved mask corresponds to the simple polar development

$$r = 50 - 10\cos\theta, \tag{3}$$

where θ corresponds to the angular position of the substrate. For $\theta = 0°$, corresponding to a substrate near the material target, the mask radius is 40 mm, which means that the substrate is completely hidden. On the opposite side ($\theta = 180°$), the mask radius is 60 mm and the substrate is completely exposed to the deposition process.

Figure 3 gives the resulting uniformity: isothickness lines, perpendicular to the thickness gradient, are perfectly circular—which is logical since all the points located on a circle (centered on the rotation axis) are coated identically during one complete turn. As a consequence, this simple masking technique is appropriate only for graded coatings devoted to linear array detectors—with the major advantage that many samples can be produced at the same time since all the substrates located on the same rotation radius of the substrate holder are identically coated.

As expected, the thickness ratio between the two sides of the coating is approximately equal to 2. Notice that the thickness gradient is not constant. This is due to the mask shape that was used for this calculation and which, ideally, should be defined taking into account the natural thickness nonuniformity of the deposition chamber [10].

4. Deposition of Linear Variable Filters Using a Translation Movement

To obtain straight isothickness lines, as required for matrix detectors, the main idea was to use a translation movement of the mask in front of the substrate. As shown in Fig. 4, we can consider two geometric approaches. Notice that the translation direction is the same in both cases.

In the first case, Fig. 4(a), the mask is formed with a simple metallic blade with a straight edge and the translation length is equal to the substrate length. According to Fig. 4(a), the right side of the substrate is longer exposed to the deposition process than the left side. Ideally, the thickness gradient is, therefore, parallel to the translation direction and isothickness lines are thus parallel to the mask edge. The great advantage of this approach is that the thickness gradient is directly connected to the translation speed. Using a stepper motor, the thickness gradient can be easily programmed.

However, due to the natural nonuniformity of the deposition process, isothickess lines are not perfectly straight and the transverse nonuniformity, perpendicular to the translation direction, is, in fact, given

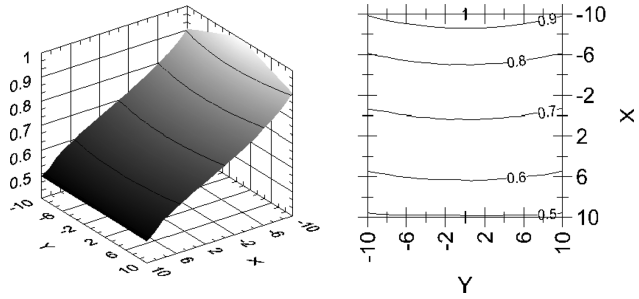

Fig. 3. Calculated uniformity of a linear variable filter deposited with a static mask and a rotating substrate. Isothickness lines are circular, the center corresponding to the rotation axis of the substrate holder.

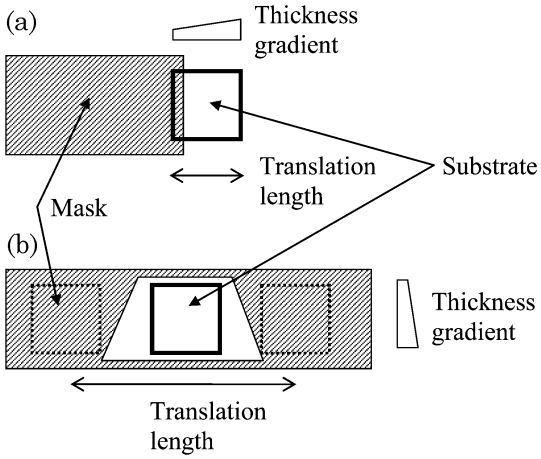

Fig. 4. Two possible geometries for producing linear variable filters with a translation movement. (a) The translation is limited to the length of the substrate; the thickness gradient is linked with the translation speed and aligned with the movement. The result is sensitive to the deposition process uniformity. (b) The translation length must be long enough to hide the substrate behind the mask on both sides; the thickness gradient is linked to the length of the mask and perpendicular to the movement direction. In case the mask is fixed and the translation is applied to the substrate, isothickness lines are perfectly straight.

directly by the nonuniformity of the deposition process itself.

In the second case, Fig. 4(b), the mask is formed with a trapezoid window and the translation is long enough to hide the substrate behind the mask on both sides [6]. Assuming this translation is performed with a uniform speed, the deposited thickness for each point is, therefore, proportional to the length of the window along the movement direction. As a result, the thickness gradient is linked to the shape of the window. Contrary to the previous case, the thickness gradient is now perpendicular to the movement direction, while isothickness lines are parallel to it. As previously, the natural thickness nonuniformity of the deposition process might have some impact on this ideal result. However, this difficulty can be completely canceled if we consider a static mask with the translation movement applied to the substrate itself. In that case, indeed, two points of the substrate aligned with the translation direction will undergo the same effects at the same positions inside the deposition chamber (with only a time delay) and will, consequently, be coated identically (assuming a constant translation speed and deposition rate), even if the deposition process is not uniform.

As a result, isothickness lines can be perfectly straight, whatever the thickness distribution of the deposition machine. This is the major advantage of this second geometric approach, when such a result cannot be strictly obtained with the first one.

To sum up, these two approaches show complementary advantages and drawbacks. The first one is more flexible with the help of a stepper motor, provides the highest possible deposition rate since one extremity of the substrate is never hidden, but is not able to give perfectly straight isothickness lines. On the contrary, the second can give perfectly straight isothickness lines, but requires a specific mask for each intended thickness gradient and provides a much slower deposition rate since the substrate is completely hidden at both extremities of the translation movement.

In both cases, it should be pointed out that the deposition process thickness uniformity must be taken into account to achieve the right thickness gradient on the substrate. As a consequence, the translation speed for the first system [Fig. 4(a)] or the mask shape for the second one [Fig. 4(b)] will depend on the location of the system inside the deposition chamber. The manufacturing of several identical coatings during a single deposition run thus requires as many specific masking systems, which is not convenient at all. For this reason, linear variable filters for 2D array detectors are usually manufactured one at a time.

5. Deposition of Linear Variable Filters Using Both Rotation and Translation Movements

We presented in Section 3 a masking system based on a rotation movement that is able to produce several identical linear variable filters, but these filters are not suited for 2D array detectors because of poor transverse uniformity perpendicular to the thickness gradient. On the other hand, we presented in Section 4 masking systems based on a translation movement that are able to produce linear variable filters for 2D array detectors, but only one at a time.

In this section, the idea is thus to combine both the rotation and the translation movements with the aim of manufacturing, in a single deposition run, several linear variable filters with a transverse uniformity that is compliant with 2D array detector requirements. The mechanical system we developed is illustrated in Fig. 5. Substrates are classically placed on a rotating substrate holder. Each of them is covered with a mask mounted on its own translation stage attached to the rotating substrate holder. The motion of these masks is induced by the rotation of the substrate holder itself, inside a came fixed within the deposition chamber. During the deposition, samples are exposed to the natural thickness distribution of the deposition chamber with a 2π periodic modulation due to the rotation of the substrate holder. As an example, Fig. 6 shows the angular deposition rate distribution curves corresponding to rotation radii respectively equal to 40, 50, and 60 mm, which correspond to the internal, central, and external rotation radii for a 20 mm square sample centered on the 50 mm rotation radius. As stated in Section 2, the natural thickness distribution has a symmetrical plane defined by the center of the material target and the rotation axis. The maximum thickness is deposited near the target ($\theta = 0°$) and the minimum on the opposite side ($\theta = 180°$). Since the masks are rotating with the substrate holder, this thickness

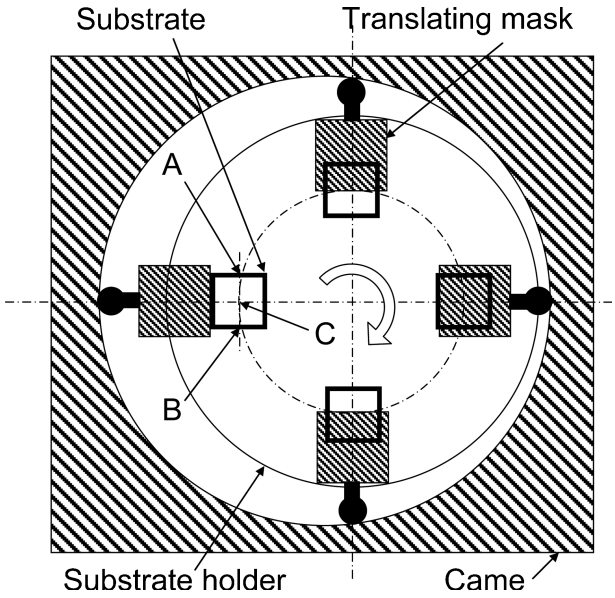

Fig. 5. Representation of a mechanism combining a translation movement of the mask with the rotation of the substrate. The translation is induced by the rotation by the mean of an external came.

distribution is modulated with the same periodicity by the translation movement of the masks induced by the came.

We then looked for the conditions that allow obtaining the best uniformity perpendicular to the translation movement. For this purpose, we considered the central point, C, of the substrate and the line originating from it, tangential to the substrate motion direction and consequently perpendicular to the mask translation direction. Let us consider A and B as the two points of this line corresponding to the substrate extremities, as illustrated in Fig. 5. Notice that A and B are located on the same rotation radius, i.e., 50.99 mm, while this radius is a bit shorter for point C, i.e., 50 mm. As a consequence, without any mask, points A and B receive the same amount of material during one revolution. To illustrate this point, Fig. 7 shows the angular deposition rate distribution for these two points. The two curves are identical with an angular shift of 22.62° that corresponds to the angular separation of points A and B. According to its position, the mask will allow or not the deposition on the substrate and, since the [AB] line is parallel to the edge of the mask, points A and B are coated simultaneously. The final amount of material that is deposited on these points is given by the summation of the curves over the angular sectors corresponding to the open positions of the mask. Supposing the mask is only open during the $\Delta\theta_1$ angular sector represented in Fig. 7, it clearly appears that the deposited thickness is more important for point B than for point A. To compensate for this thickness imbalance, it is necessary for both the mask movement and the natural thickness distribution to have the same symmetry axis, as represented by the $\Delta\theta_2$ angular sector. As a consequence, the came shape must be symmetrical and aligned with the symmetry axis of the deposition process.

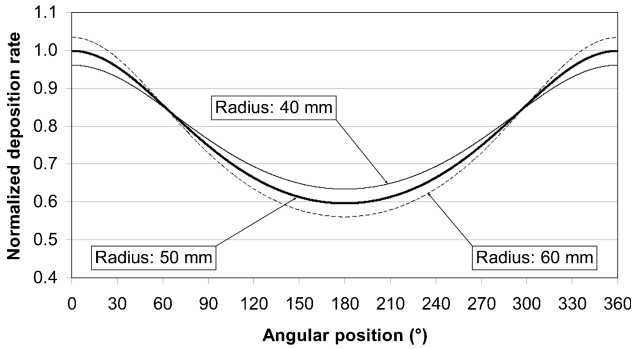

Fig. 6. Typical angular deposition rate for the internal, central, and external positions of the substrate. The deposition rate is higher closer to the material target (0°) and lower on the opposite side (180°).

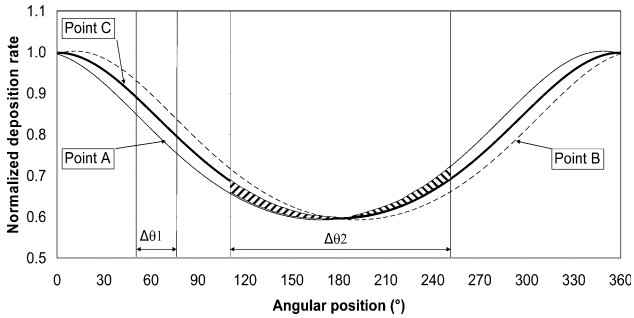

Fig. 7. Angular deposition rate for points A, B, and C of the central line (see Fig. 5). To compensate for the angular shift existing between points A and B and, thus, to deposit the same thickness of material, the mask should be open symmetrically ($\Delta\theta_2$).

Let us now consider the central point, C. The angular deposition rate distribution curve corresponding to this point is also given in Fig. 7 and can be compared with the curve corresponding to point A. These curves are not exactly identical since these two points are not located on the same rotation radius and the angular shift between the two curves is half what it was before, 11.31°. However, one can notice that these two curves intersect at about $\theta = 180°$, which tends to balance the thickness amount for these two points when the mask is open symmetrically, as illustrated by the two hatched areas in Fig. 7. As a result, the deposited thickness is almost the same for points A, B, and C; isothickness lines are almost straight, perpendicular to the thickness gradient.

To illustrate the efficiency of this solution, we performed a calculation for the masking mechanism represented in Fig. 8. The location of the edge of the mask, which can be regarded as the came shape, is given by the polar development

$$r = 60 - 20\cos\theta. \quad (4)$$

For $\theta = 0°$, corresponding to a substrate near the material target, the mask radius is 40 mm, which means

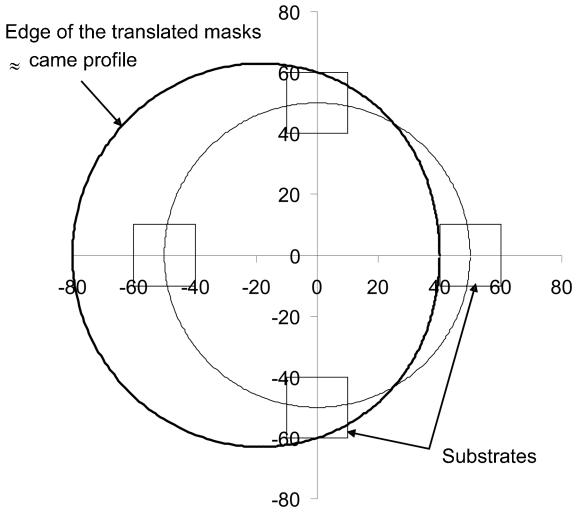

Fig. 8. Definition of a masking geometry combining a translation of the mask with the rotation of the substrate for the deposition of linear variable filters. The position of the edge of the mask can be regarded as the came shape. The rotating substrate is progressively hidden during half a turn.

that the substrate is completely hidden. For $\theta = \pm 90°$, the mask radius is 60 mm, so that the mask is completely open during half a turn. This way, the internal side of the substrate is always exposed to the deposition process while the external side is hidden half the time, which should result approximately in a factor of 2 thickness ratio between the two sides.

Figure 9 gives the resulting uniformity. As expected, isothickness lines are straight. The thickness ratio is a bit higher than 2, and the thickness gradient is not perfectly constant. As previously said, the gradient profile is due to the fact that the came shape was defined very simply, without taking into account the natural thickness nonuniformity of the deposition chamber. More precisely, the minimum and maximum thickness uniformity calculated for the internal, central, and external lines are given in Table 2. Perpendicular to the thickness gradient, the maximum thickness is obtained for the central point (C), while the minimum thickness is obtained for the extreme two points (A and B). From these results, one can estimate that the transverse uniformity for a 20 mm length is higher than 0.998, even very close to 0.999.

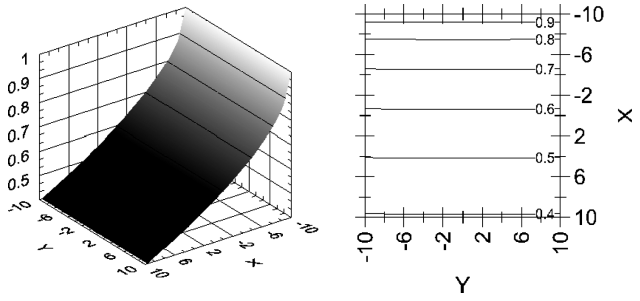

Fig. 9. Calculated uniformity of a linear variable filter deposited with a masking mechanism combining the translation of the mask with the rotation of the substrate. Isothickness lines are almost straight, with a transverse uniformity higher than 0.998 over a 20 mm length.

Table 2. Transverse Uniformity Calculated for the Internal, Central, and External Lines for a Linear Variable Coating Manufactured Using Both a Translation and a Rotation Movement in the Masking Mechanism

	Normalized Minimum Thickness	Normalized Maximum Thickness	Transverse Uniformity
Internal line	0.99883	1.00000	0.99883
Central line	0.58591	0.58636	0.99923
External line	0.39340	0.39383	0.99890

It should be pointed out that this result is mainly due to the masking mechanism itself, and not linked to the definition of the came shape or to the geometry of the deposition process (main sputtering direction and directivity). For a given deposition chamber, this means that the main work will consist in defining the came shape that gives the expected thickness gradient, a high transverse uniformity being naturally guaranteed by the mechanism.

At last, considering a 2D array detector with about 500 lines of pixels, a transverse uniformity equal to 0.998 roughly corresponds to a one-pixel misregistration and can be considered as a required specification. From this point of view, the performance provided by this masking mechanism is fairly good.

6. Manufacturing and Measurements

To prove experimentally the ability of such a mechanism to produce linear variable filters with a high transverse uniformity, a test has been performed using a dual ion beam sputtering machine with a geometry corresponding to that presented in Section 2. This trial was performed before the characterization of the natural thickness distribution was achieved so that the came profile could not be designed accurately for a given thickness gradient. For this trial, the came shape was thus only designed to give a thickness ratio equal to 2 along a 20 mm length, assuming a uniform distribution.

A linear variable filter formed with a single cavity Fabry–Perot design ($(HL^5)\,4H\,(LH)^5, L = SiO_2, H = Ta_2O_5$) was deposited on a 20 mm square substrate. A mapping of the transmittance profile of the filter was performed on a spectrophotometer specially developed in the laboratory for localized measurements [11]. This characterization was performed on a 14 mm × 14 mm square with a 2 mm step square grid and a 200 μm light spot diameter. To prevent a misalignment between the orientation of the thickness gradient of the coating and the translation axis used for the mapping, a corrective interpolation of the measured points was applied to estimate the optimum transverse uniformity.

Table 3. Centering Wavelengths Measured on a Linear Variable Filter Manufactured using Both Translation and Rotation movements in the Masking Mechanism

		Position Along the Thickness Gradient (mm)							
		0	2	4	6	8	10	12	14
Transverse Position (mm)	0	1422.1	1319.0	1218.9	1127.0	1041.4	960.23	879.39	790.17
	2	1424.0	1320.1	1219.9	1128.0	1042.9	961.13	880.20	790.32
	4	1424.9	1320.3	1220.1	1128.1	1042.4	961.11	880.17	790.28
	6	1425.8	1321.1	1220.2	1128.1	1042.9	961.12	880.19	790.32
	8	1427.0	1322.0	1221.0	1128.3	1043.0	961.07	880.05	790.17
	10	1427.1	1322.0	1221.0	1128.2	1042.8	960.90	879.33	789.98
	12	1427.8	1322.1	1220.9	1128.1	1042.1	960.14	879.07	789.21
	14	1426.8	1320.9	1219.2	1126.9	1040.9	958.28	877.25	788.02

The measured centering wavelengths of the filter are given in Table 3. The spectral range extends from 800 to 1400 nm along 1400 mm, which corresponds to a thickness gradient that is typical of the linear variable filters we are interested in. More interesting is the transverse uniformity, given in Table 4, which is as expected most often higher than 0.998, in good agreement with simulations. It should also be noted that, surprisingly, the measured thickness distribution is slightly misaligned with the substrate axis. One possible reason for this may be a slight misalignment of the main sputtering direction with the substrate-holder rotation axis, as observed through the Ta_2O_5 thickness distribution characterization.

7. Conclusion

We have investigated the manufacturing of linear variable filters for 2D array detectors. The masking mechanism we propose, combining the translation of a metallic mask with the rotation of the substrate holder, allows answering major difficulties: obtaining a transverse uniformity higher than 0.998 and being able to produce several coatings within a single deposition run. These capabilities have been demonstrated theoretically and experimentally with good agreement. This result is mainly a characteristic of the masking mechanism, for a transverse length of 20 mm, and does not significantly depend on the deposition process geometry or the came shape.

The next step now is to adjust the came shape to obtain the right thickness gradient. For this purpose, we need to complete the characterization of the thickness distribution for the two materials involved in coatings.

Considering technical aspects, one advantage of this solution is that there is no need to introduce any motor inside the deposition chamber since the mask's motion is a consequence of the rotation of the substrate holder. On the other hand, the design of the came shape, its manufacturing, and its positioning inside the chamber are not so easy due to its large diameter, while all these points are directly linked to the thickness gradient of the variable filter. In other words, it might be time consuming to accurately achieve a prescribed thickness gradient, while a masking mechanism driven by a stepper motor is much more flexible. Moreover, in the case of linear variable filters formed with metal-dielectric bandpass structures, which are of great interest due to their extended rejection bands, the required thickness gradient is not the same for dielectric films and for metallic ones. Such a constraint would surely make our solution much more complex mechanically.

As a conclusion, compared to the solutions presented in Section 4, the masking solution we propose gives as efficient results regarding the component's optical properties, but is less flexible to implement. As a consequence, this solution is particularly interesting for its mass-production capabilities, for which the time required to optimize the system is worthwhile, while other solutions are mainly limited to unit production.

Table 4. Transverse Uniformity Measured on a Linear Variable Filter Manufactured Using Both Translation and Rotation Movements in the Masking Mechanism

		Position Along the Thickness Gradient (mm)							
		0	2	4	6	8	10	12	14
Transverse Position (mm)	0	0.9960	0.9976	0.9983	0.9989	0.9985	0.9991	0.9991	0.9998
	2	0.9974	0.9985	0.9991	0.9997	0.9999	1	1	1
	4	0.9980	0.9986	0.9992	0.9998	0.9994	1	1	1
	6	0.9986	0.9992	0.9994	0.9999	1	1	1	1
	8	0.9994	0.9999	1	1	1	0.9999	0.9998	0.9998
	10	0.9995	0.9999	1	0.9999	0.9999	0.9998	0.9990	0.9996
	12	1	1	0.9999	0.9998	0.9992	0.9990	0.9987	0.9986
	14	0.9993	0.9991	0.9985	0.9987	0.9980	0.9970	0.9966	0.9971

References

1. H. A. Macleod, "Layer uniformity and thickness monitoring," in *Thin-Film Optical Filters*, 3rd ed. (Institute of Physics, 2001), pp. 488–497.
2. A. Piegari, "Graded coatings," in *Thin Films for Optical Systems*, F. Flory, ed. (Marcel Dekker, 1995), pp. 475–519.
3. A. Piegari, M. R. Perrone, and M. L. Protopapa, "Ultraviolet-graded coatings for lasers: surface optical performance," Thin Solid Films **373**, 155–158 (2000).
4. J. P. Coates, "New microspectrometers," Spectrosc. **15**, 21–27 (2000).
5. A. Semery, "Wedge filter imaging spectrometer," presented at the Sixth International Conference on Space Optics (ICSO 2006), Noordwijk, Nederland, 27–30 June 2006).
6. A. Piegari and J. Bulir, "Variable narrowband transmission filters with a wide rejection band for spectrometry," Appl. Opt. **45**, 3768 (2006).
7. F. Villa and O. Pompa, "Emission pattern of a real vapor sources in high vacuum: an overview," Appl. Opt. **38**, 695–703 (1999).
8. Y. Yamamura and N. Itoh, "Sputtering yield," in *Ion Beam Assisted Film Growth*, T. Itoh, ed., Beam Modification of Materials (Elsevier, 1989), Vol. 3, pp. 59–100.
9. E. Vireton, P. Ganau, J. M. Mackowski, C. Michel, L. Pinard, A. Remillieux, and P. Laprat, "SiO2-Ta2O5 sputtering yields: simulated and experimental results," Nucl. Instrum. Methods Phys. Res. B **95**, 34–40 (1995).
10. L. Pekker, "Using calibration tests for adjusting target uniformity masks," Thin Solid Films **474**, 211–216 (2005).
11. L. Abel-Tiberini, F. Lemarquis, and M. Lequime, "Dedicated spectrophotometer for localized transmittance and reflectance measurements," Appl. Opt. **45**, 1386–1391 (2006).